

Design and Fabrication of Micro Optical Film by Ultraviolet Roll Imprinting

Suho AHN, Minseok CHOI, Hyungdae BAE, Jiseok LIM, Ho MYUNG, Hongmin KIM, and Shinill KANG

Nanoreplication and Microoptics National Research Laboratory, Yonsei University, Seoul 120-749, Korea

(Received January 17, 2007; revised April 3, 2007; accepted April 6, 2007; published online August 23, 2007)

With increasing demand for large-scale functional optical films with microstructure in the field of flat panel displays, a technology capable of fabricating large-scale polymeric micro-patterns has received much attention. To fabricate large-area micro-optical films, we designed and constructed an ultraviolet roll imprinting system consisting of a roll stamp, a material dispensing unit, a pair of flattening rollers, a contact roller, and a releasing roller. Two methods for fabricating roll stamps were considered: direct machining of the roll base and wrapping a flat stamp around the roll base. As practical examples of the roll imprinting process, we designed and fabricated a lenticular lens array, a pyramidal pattern, and a microlens array, and measured and analyzed their geometrical and optical properties. Our results suggest that the proposed UV roll imprinting process is a feasible method for mass producing large-scale functional optical films. [DOI: [10.1143/JJAP.46.5478](https://doi.org/10.1143/JJAP.46.5478)]

KEYWORDS: UV roll imprinting, large scale optical film, lenticular lens, pyramid pattern, microlens array

1. Introduction

Flat panel displays are now key components in devices such as compact televisions, large screen televisions, personal computers, portable information devices, and so on. Efforts to produce improved displays are driven by demand for high definition displays of low weight and thin feature size, with improved brilliancy and lower power consumption. In flat panel displays, various functional optical films, including lenticular lens sheets, prism sheets, diffusion films, and microlens arrays (MLAs), are used to improve the optical performance. To attain the optical performance required for display applications, the microstructure in functional optical films must be fabricated accurately. At present, functional optical films are generally fabricated by a polymer laminating process and repeated printing on the substrate film. However, a polymer replication process using a precisely machined mold would be more suitable for the mass production of functional optical films with highly accurate microstructure.¹⁾ The hot embossing process has the potential to produce high quality microstructure in optical films, but the heating and cooling times of the mold and material involved in this process make the cycle time too long for commercial applications.²⁾ A UV imprinting process is regarded as the most suitable process for producing functional optical films with microstructure, because the cycle time is very short and microstructure can be replicated with high precision. In addition, the UV imprinting process provides components with low thermal expansion, enhanced stability, and low birefringence. Moreover, this process has the advantage of accurate pitch tolerance due to negligible lateral shrinkage of the molded part.^{3–6)}

In efforts to fabricate functional optical films for flat panel displays, the development of large-scale fabrication technology is a priority.⁷⁾ Screen size is of the utmost importance in the competitive display market, and large screens require a fabrication technology capable of producing large-scale functional optical films. Furthermore, the ability to fabricate large-scale optical films would offer incredible economies of scale. Display manufacturers would be able to produce a greater number of products from a single sheet, thereby increasing efficiency. To attain the performance and production size of functional optical films required for display

applications, a UV-molding system for large-scale optical films is required. In the conventional UV-molding process, a flat mold is used. Hence, in efforts to develop a large scale UV-molding process, developing a large scale flat mold is a natural starting point. However, machining large scale flat molds is very difficult, and the machining costs increase exponentially with increasing mold size.⁸⁾ Furthermore, previous efforts to use a UV-molding process to fabricate large-scale optical films have encountered uniformity and releasing problems. To overcome these financial and fabrication issues associated with developing a UV-molding process for fabricating large-scale functional optical films, a UV roll imprinting process that uses a roll stamp was developed.⁹⁾ This process was found to have several advantages for fabricating large-scale functional optical films, such as good releasing, easy control of defects, and high uniformity. Furthermore the UV-roll imprinting process is suitable for mass production because it is an in-line process.

In the present study, we used a UV roll imprinting system consisting of a roll stamp, material dispensing unit, a pair of flattening rollers, a contact roller, and a releasing roller.⁹⁾ Two methods for fabricating the roll stamp were considered: direct machining of the roll base and wrapping a flat stamp around the roll base. As practical examples of the roll imprinting process, a lenticular lens array, a pyramidal pattern and an MLA were designed and fabricated, and their geometrical and optical properties were measured and analyzed.

2. Experimental Methods

2.1 Mold fabrication

In the UV-roll imprinting process for functional optical films, fabrication of the roll stamp is very important because the dimensional accuracy and uniformity of the roll base and mold cavity determine the properties of the functional optical film. Various methods can be used to fabricate the roll stamp, including direct mechanical machining of the roll base and wrapping a thin metal or polymer stamp around the roll base. Direct mechanical machining of the roll base is a simple process, and can produce highly accurate microcavity patterns without any joining line on the stamp. The wrapping of a thin metal or polymer stamp around the roll base can be

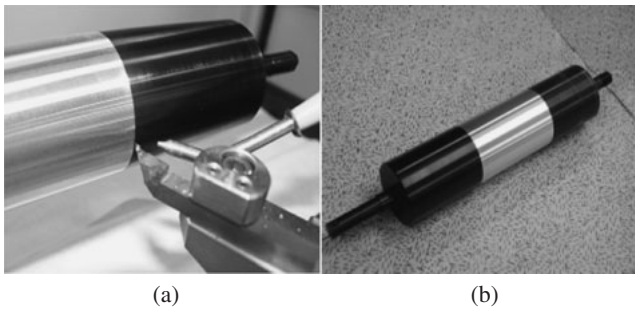


Fig. 1. Images of (a) the tooling process using the two-axis CNC diamond machining system, NANOFORM[®] 200, and (b) a machined aluminum roll stamp of length 210 mm, diameter 50 mm, and patterned length 80 mm.

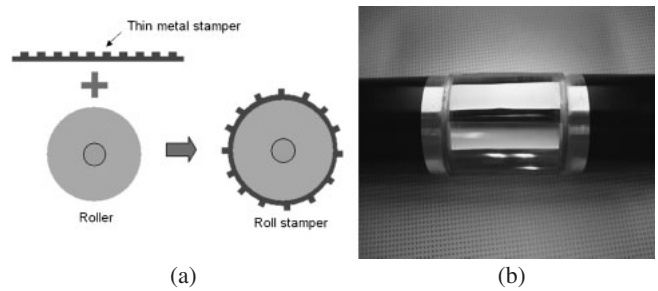


Fig. 3. (a) Schematic diagram of the process flow for the roll stamp: A thin metal stamp was fabricated by applying an electroforming process to the machined convex pyramid pattern. The electroformed thin metal stamp with a thickness of 210 μm was then wrapped around the aluminum roll base. (b) Image of a manufactured roll stamp with length 210 mm and diameter 50 mm.

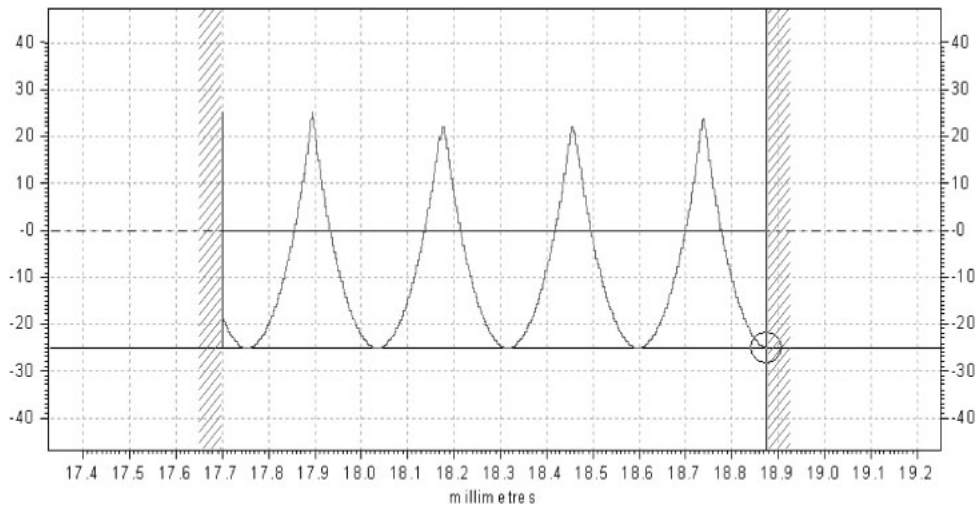


Fig. 2. Surface profile of the machined cavity for lenticular lenses with a pitch of 280 μm , a radius of curvature of 223 μm , and a sag height of 47 μm . The deviation of the sag height of the lenticular lenses from the mean value in the measured points was less than 0.5 μm .

used to produce patterns with various shapes, which can be fabricated by various micro- and nanopatterning processes on the thin stamp. In this study, we used the following approaches: a directly mechanically machined roll stamp in the fabrication of a lenticular lens sheet; a thin metal stamp with a pyramid pattern wrapped around the roll stamp; and a polymer stamp with for MLA wrapped around the roll stamp.

2.1.1 Direct machining on the roll

To fabricate roll stamps for producing a lenticular lens sheet with a pitch of 280 μm , a sag height of 50 μm , and a radius of curvature of 223 μm for wide viewing angle, we carried out a precision mechanical machining process using a diamond tip on an aluminum roll base. Figures 1(a) and 1(b) show an image of the tooling process and a machined aluminum roll stamp of length 210 mm and diameter 50 mm respectively. The patterning width of the roll stamp was 80 mm. Figure 2 shows the surface profile of the machined cavities for the lenticular lenses measured using a mechanical surface profiler with a Z-directional resolution of 0.8 nm. The measured pitch and sag height of the lenticular lens cavity array were 280 and 47 μm , respectively. Due to the shaping error, the sag height of the lenticular lens mold was 3 μm less than the design value. However, among the

points we measured using the surface profiler, the deviation of the sag height from the mean value of 47 μm did not exceed 0.5 μm , indicating that the direct mechanical machining process used here had good uniformity.

2.1.2 Nickel electroforming after machining

To fabricate a roll stamp for producing a pyramid pattern with pitch 50 μm and height 25 μm , a thin metal stamp was wrapped around the roll base, as depicted in Fig. 3(a). To fabricate the thin metal stamp, a master pattern with the final pyramid shape was first fabricated by machining a V-groove pattern on a flat specimen, rotating the specimen by 90°, and then machining another V-groove pattern. The thin metal stamp was then fabricated by applying an electroforming process to the mother pattern. After the electroforming process, the backside of the stamp was polished to obtain a mirror surface and uniform thickness. The electroformed thin metal stamp with a thickness of 210 μm was then wrapped around the aluminum roll base. Figure 3(b) shows the thin metal stamp wrapped around the roll base. The outer size of the roll stamp was the same as that of the directly machined roll stamp described above. Figure 4 shows scanning electron microscopy (SEM) images of the concave pyramidal cavities with pitch 50 μm and depth 24 μm on the

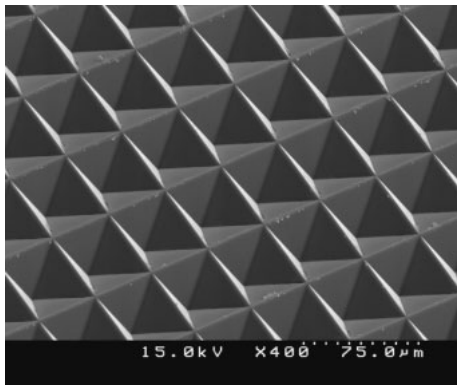


Fig. 4. SEM image of concave pyramidal cavities with pitch 50 μm and depth 24 μm on a thin metal stamp.

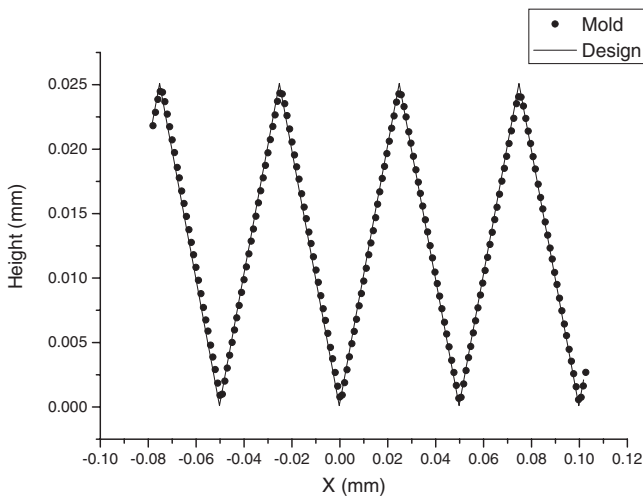


Fig. 5. Comparison of the designed and measured surface profiles of the concave pyramidal cavities.

thin metal stamp. Figure 5 shows the designed surface profile and the profile measured using the surface profiler; the small difference between the designed and measured profiles can be attributed to measurement error and master shaping error.

2.1.3 Polymer replication after micro-photolithography

Recently, MLAs have been widely used in various applications, such as fiber coupling, light gathering and light extraction;¹⁰⁻¹⁴⁾ therefore, many fabrication methods have been developed.¹⁰⁻¹⁴⁾ Among these techniques, the thermal reflow process generates microlenses whose surface contours are closest to a spherical shape, which is important for light extraction from planar light sources, whereas the lithographic, galvanofarming and abfarming (LIGA) process is the most effective and economical for the mass production of MLAs. Therefore, a method that combines the thermal reflow and LIGA processes seems to be a good choice for fabricating MLAs.¹⁵⁾

To fabricate an MLA roll stamp, we fabricated the master pattern by a photolithography and reflow process and then fabricated the thin polymer stamp by replicating the master pattern using silicone urethane acrylate photopolymer. The sag height of the reflowed microlens was 1.2 μm, and the rectangular base size was about 4.8 × 4.8 μm². Figure 6 shows an SEM image of the MLA polymer stamp.

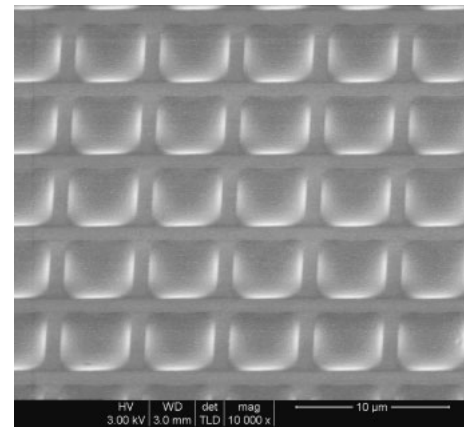


Fig. 6. SEM image of concave square MLA cavities with pitch 5.6 μm and depth 1.2 μm on a flexible polymer stamp. The master pattern was fabricated by a photolithography and reflow process, and the thin polymer stamp was fabricated by replicating the master pattern using silicone acrylate photopolymer.

2.2 System construction and process establishment

To replicate large-scale functional optical films with high-quality microstructure, a continuous UV roll imprinting system was designed and constructed.⁹⁾ Figure 7 shows a schematic diagram of the UV-roll imprinting system. The system was equipped with a dispensing system that coated a UV-curable photopolymer on a transparent film substrate; a pair of flattening rollers for uniform coating of the photopolymer on the substrate; a roll stamp that had the inverted shape of the designed microstructures; a contact roll for bringing together the film substrate and the roll stamp; a UV exposing unit consisting of a UV lamp, reflector, aperture and shutter; and a releasing roller which released the imprinted functional optical film from the roll stamp. In the dispensing system, the coating thickness was controlled by the ejection pressure, needle size, photopolymer viscosity, the feed rate of the substrate film, and so on. The flattening roller could be used to uniformly coat the material on the substrate film by controlling the gap size between the rollers. In the contact roller, a passive gap control system was used to control the thickness of the final replica by varying the pressure of contact of the contact roller with the substrate and indirectly with the roll stamper. A contact force of 90.6 N was applied to increase thickness uniformity as explained in the previous paper.⁹⁾ The substrate film that had been coated with UV-curable photopolymer passed through the roll gap, so that the microstructure on the roll stamp was transferred to the material. At the same time, the resin was cured by UV irradiation from the UV-exposing system, so that functional optical films were formed. In the UV-exposing system, a metal halide UV-lamp with a power of 80 W/cm² and a wavelength range of 265–420 nm was used in conjunction with an ellipsoidal reflector designed to collimate the UV light. The aperture size of UV-exposure system was 20 × 200 mm² and the irradiated intensity at the aperture plane was 200 mW/cm². To apply sufficient UV-energy to the photopolymer, the rotation speed of the roll stamper was selected as 5 rpm (imprinting speed was about 785 mm/min), in which the UV-exposing dose was about 300 mJ/cm².^{9,16)} The fabrication throughput can be improved significantly by increasing the power of the UV

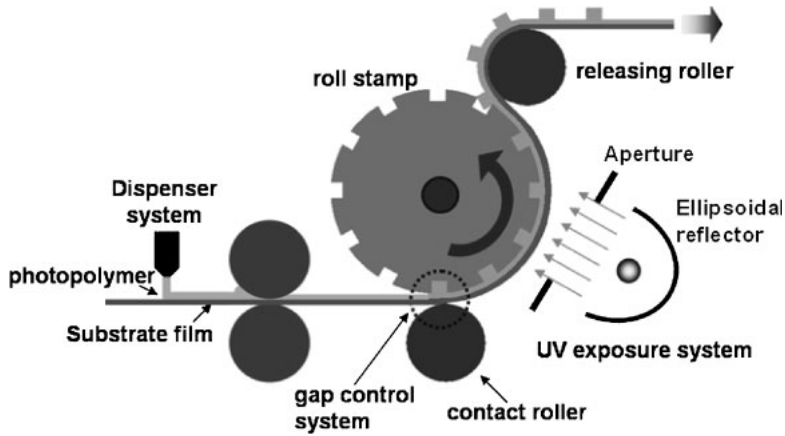


Fig. 7. Schematic diagram of the UV roll nano-imprinting system for a flexible substrate. This system is suitable for the replication of large-scale nano- and micropatterns.

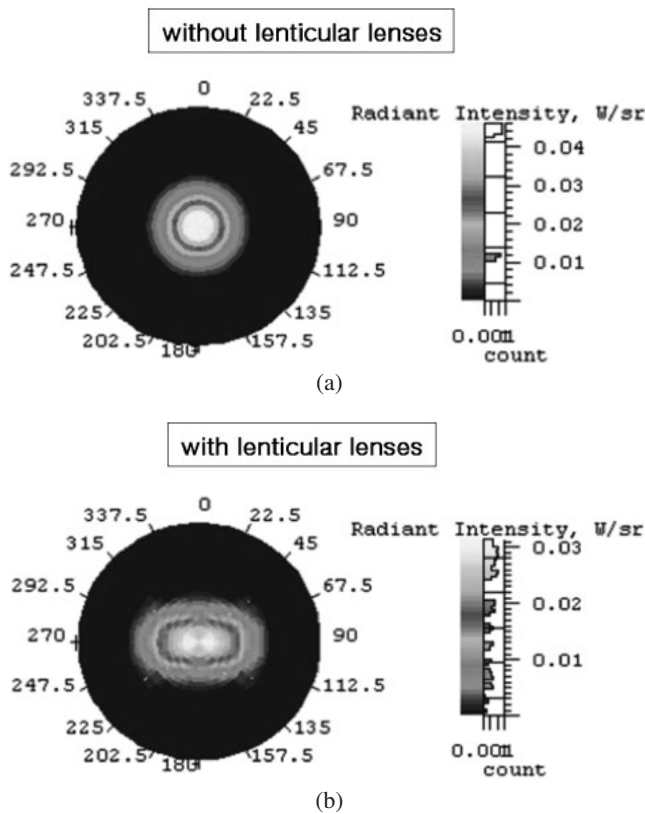


Fig. 8. Simulated radiant intensity results of the source (a) without the lenticular lens sheet, and (b) with the lenticular lens sheet, in a 2D polar style raster chart.

lamp, diameter of the roll stamper and the size of the aperture of exposure system. The rotation velocities of the roll stamp and the other rollers were controlled by a stepping motor and gear system. An adhesion promoter-coated poly(ethylene terephthalate) (PET) film of thickness 250 μm was used for the substrate film, and a urethane acrylate photopolymer was used for the molding material. The photopolymer had a refractive index of 1.52 at a wavelength of 587.6nm and a viscosity of 300 cP at 25 $^{\circ}\text{C}$.

3. Imprinting Results

3.1 Lenticular lens sheet for projection screens

In projection displays, the light through the screen is typically brightest normal to the screen, and then gradually falls off in brightness as the viewer moves away from normal

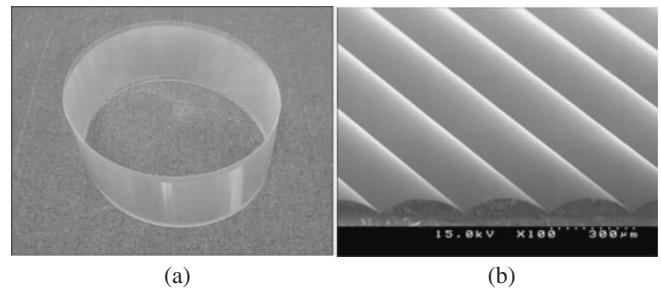


Fig. 9. Fabrication results: (a) image of the roll imprinted lenticular lens sheet on a PET substrate with a width of 80mm, and (b) SEM image of the roll imprinted lenticular lenses with a pitch of 280 μm , a depth of 47 μm , and a radius of curvature of 223 μm .

to the screen. This decrease typically follows a Gaussian or normal distribution. The viewing angle of a display is usually defined as the angle at which the brightness is half the maximum brightness. To increase the viewing angle, a lenticular lens sheet can be mounted on the projection screen. In this study, a lenticular lens array that would yield a viewing angle of 40 $^{\circ}$ was designed by optical simulation software. The designed pitch, sag height and radius of curvature of this lenticular lens array were 280, 50, and 223 μm , respectively. Figure 8 shows the simulated radiant intensity distribution of the source (a) without and (b) with the lenticular lens array.

A lenticular lens sheet was fabricated by the present continuous UV-roll imprinting process using a roll stamp with concave lens cavities with a pitch of 280 μm , a depth of 47 μm and a radius of curvature of 223 μm . The size of fabricated optical film was 150mm wide and 1m long and the patterned area was 80mm wide and 1m long. Figure 9 shows (a) an image of the roll imprinted lenticular lenses, and (b) an SEM image showing the cross section of the lens sheet. In addition, to quantify the replication quality of the roll imprinted lenticular lenses, we measured the surface profile of the imprinted lenses and compared it with the surface profile of the roll stamp (Fig. 10).⁹⁾ The mean depth of the lens cavities was 47 μm and the mean sag height of imprinted lenses was 43 μm , which can be attributed to limitations of the mechanical profiler in measuring sharp concave edges. It is clear from Figs. 9 and 10 that the lens surface quality is very good and that the edges are sharp. To evaluate the optical performance of the imprinted lenticular lens array, a normalized intensity distribution of the light

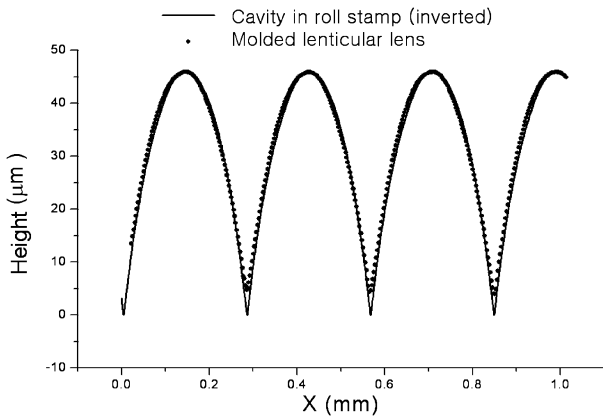


Fig. 10. Comparison of the surface profiles of the mold cavities and the UV roll imprinted lenticular lenses. The mean depth of lens cavities was $47\ \mu\text{m}$ and the mean sag height of the imprinted lenses was $43\ \mu\text{m}$; the discrepancy between cavity depth and sag height is due to limitations of the mechanical profiler in measuring sharp concave edges.

passing through the lenticular film was measured with varying the viewing angle in the vertical and horizontal directions, and was compared with that from the light source, as depicted in Fig. 11. The intensity distribution in the vertical direction was similar to that of the light source, and the viewing angle in the horizontal direction with the lenticular lens film was 43° . These results are similar to the simulated values, indicating that the imprinted lenticular lens array satisfies the design specification.

3.2 Optical film with pyramid micropatterns

A functional optical film with a pyramid pattern of pitch $50\ \mu\text{m}$ and height $25\ \mu\text{m}$ for bright enhancement of liquid crystal display (LCD) backlight unit was designed and fabricated using the present UV-roll imprinting process with a thin metal stamp wrapped around a base roll. The size of imprinted optical film was $150\ \text{mm}$ wide and $1\ \text{m}$ long and the patterned area was $60\ \text{mm}$ wide and $1\ \text{m}$ long. Figure 12 shows an SEM image of the UV roll imprinted pyramid pattern. The surface quality and edge sharpness of the pattern are very high. Figure 13 shows a comparison of the inverted surface profile of the pyramid cavities and the surface profile of the imprinted pyramid pattern. The deviation of the surface profiles between the cavity and imprinted patterns was less than $0.05\ \mu\text{m}$, indicating excellent replication. The measured pitch and height of the imprinted pattern were 50 and $24\ \mu\text{m}$, respectively. Hence the pitch of the imprinted pattern is the same as the design value, but the height is $1\ \mu\text{m}$ less than the design value; this discrepancy was mainly caused by machining error in the master patterning and electroforming process. To evaluate the optical properties of UV-roll imprinted brightness enhancement films, the radiant intensity distribution in a two-dimensional (2D) polar style raster of backlight unit with pyramid pattern film was measured and compared with that without pyramid pattern film. The test set-up composed of reflector, lamp, diffuser plate, pyramid pattern film and receiver was used for the measurement. Figures 14(a) and 14(b) show the measured radiant intensity results of backlight unit without and with pyramid pattern film, respectively. The measured maximum brightness of backlight unit without pyramid pattern film was $5239\ \text{cd}$ and that with pyramid pattern film was $6834\ \text{cd}$. It is

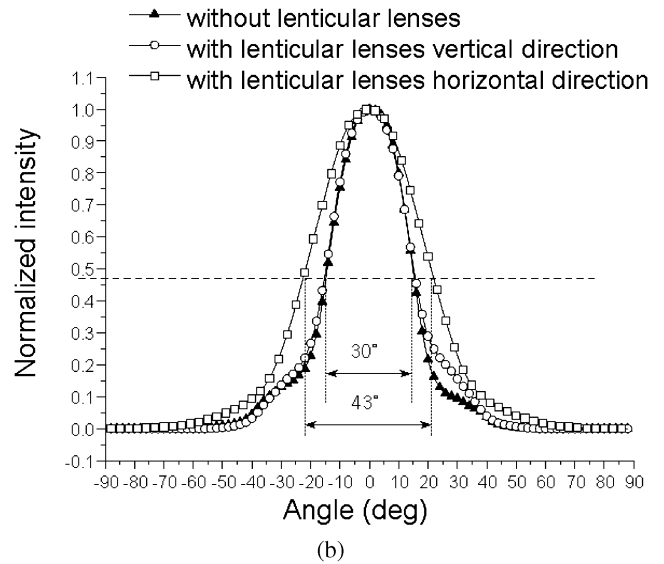
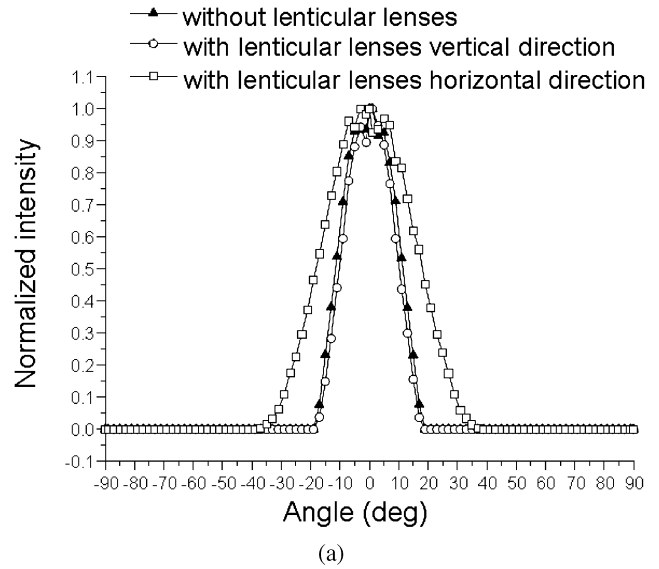


Fig. 11. Normalized intensity profile without lenticular lenses and with lenticular lenses in two directions: (a) simulation results and (b) measurement. The intensity distribution in the vertical direction was similar to that of the light source and the viewing angle in the horizontal direction with the lenticular lens sheet was 43° . These characteristics are similar to the simulated values.

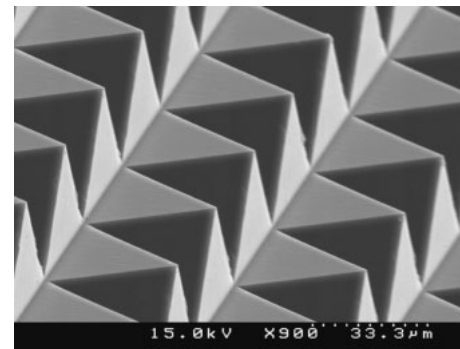


Fig. 12. SEM image of the UV roll imprinted pyramid pattern with pitch $50\ \mu\text{m}$ and height $24\ \mu\text{m}$.

noted that the maximum brightness is increased about 30% and a concentrated viewing angle can be obtained by applying the pyramid pattern film.

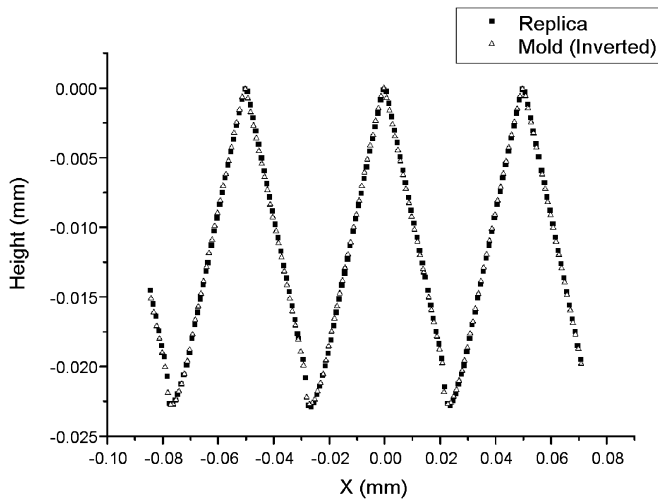


Fig. 13. Comparison of the inverted surface profile of the pyramid cavities and the surface profile of the imprinted pyramid pattern. The deviation between the cavity and imprinted pattern surface profiles was less than 0.05 μm .

3.3 Optical film with square MLA

In flat panel displays, MLAs are used for diverse purposes. For example, MLAs can be used instead of the bumpy reflector that is used in reflective LCDs (RLCDs) to eliminate the specular reflection that leads to a poor contrast ratio. Specifically, an MLA wrapping on the device serves as a “bumpy transmitter” that redirects the propagation direction of both incident and exit beams, rendering a viewing characteristic that is more symmetric than can be achieved using a conventional bumpy reflector structure.¹⁶⁾ A optical film having microlens arrays with a lens base size of $4.8 \times 4.8 \mu\text{m}^2$, lens pitch of $5.6 \mu\text{m}$, and array size of 1000 by 1320 was fabricated by the continuous roll-imprinting process. The size of imprinted optical film was 150 mm wide and 1 m long and the patterned area was 60 mm wide and 1 m long. The microlenses fabricated in the present work by the UV roll imprinting process had a sag height of $1.2 \mu\text{m}$, and the deviation of the master and imprinted pattern was less than $0.02 \mu\text{m}$. Figure 15 shows an SEM image of the UV roll imprinted MLA and Fig. 16 shows a comparison of the inverted surface profile of the microlens cavities and the surface profile of the imprinted MLA pattern. These findings indicate that the UV roll

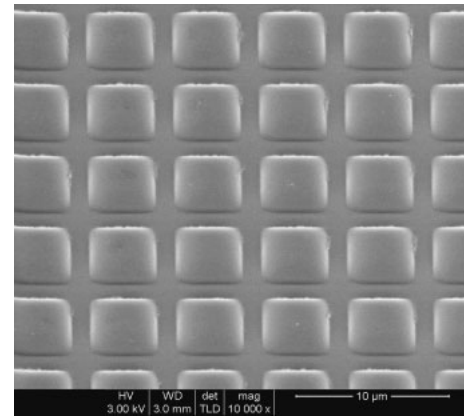


Fig. 15. SEM images of the UV roll imprinted MLA with pitch $5.6 \mu\text{m}$ and height $1.2 \mu\text{m}$.

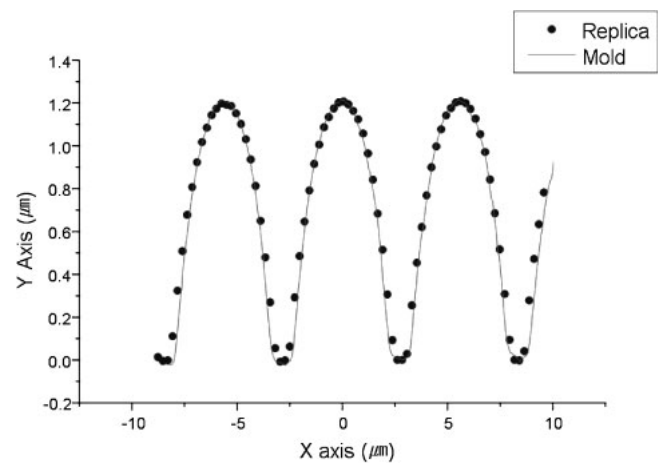


Fig. 16. Comparison of the inverted surface profile of the MLA cavities and the surface profile of the imprinted MLA. The sag height of the microlenses was $1.2 \mu\text{m}$ and the deviation between the master and imprinted patterns was about $0.1 \mu\text{m}$.

nanoimprinting process is a feasible alternative solution for the mass production of MLAs.

4. Conclusions

In this study, a UV roll imprinting system was used for fabricating large-scale functional optical films. As practical examples, a lenticular lens sheet for increasing the viewing

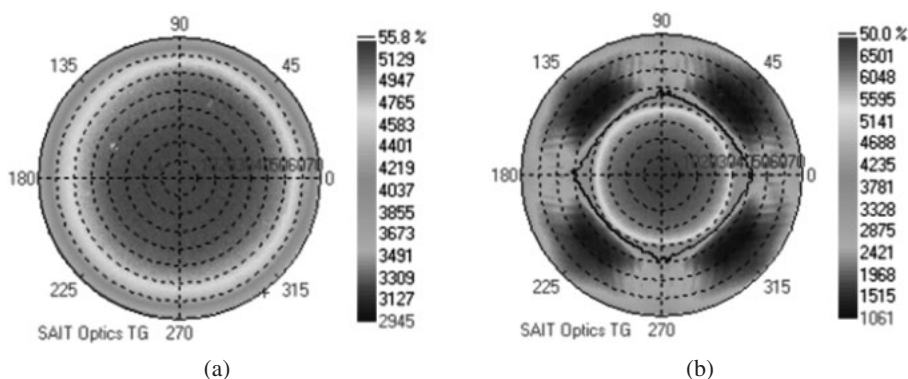


Fig. 14. Comparison of measured radiant intensity results in a 2D Polar style raster chart between (a) backlight unit without pyramid pattern film and (b) that with pyramid pattern film.

angle of a projection display, a functional optical film for an LCD backlight unit, and an MLA film were fabricated. In these example systems, the roll stamp was fabricated by a direct machining process for the lenticular lens sheet, and by wrapping a thin stamp around the roll base for the pyramid pattern and MLA. The parameters of the UV-roll imprinting process were selected for high replication quality without any defects, uniformity and production rate. A lenticular lens array with a pitch of 280 μm and a sag height of 47 μm was fabricated. The form error of the fabricated lenticular lens array compared with the design value was less than $\pm 0.3 \mu\text{m}$. The fabricated film with a pyramid pattern and an MLA had form errors of less than 0.05 and 0.02 μm , respectively. The present results suggest that our UV roll imprinting process is a feasible method for fabricating large-scale functional optical films.

Acknowledgement

This work was supported by the Korea Science and Engineering Foundation (KOSEF) grant funded by the Korea government (MOST) (No. R0A-2004-000-10368-0).

- 1) S. Kang: *Jpn. J. Appl. Phys.* **43** (2004) 5706.
- 2) N. Lee, Y. Kim, S. Kang, and J. Hong: *Nanotechnology* **15** (2004) 901.
- 3) S. Kim, D. Kim, and S. Kang: *J. Micro/Nanolithogr. MEMS MOEMS* **2** (2003) 356.
- 4) C. Decker: *Pigment Resin Technol.* **30** (2001) 278.
- 5) M. Bender, M. Otto, B. Hadam, B. Vratzov, B. Spangenberg, and H. Kurz: *Microelectron. Eng.* **53** (2000) 233.
- 6) P. Nussbaum, I. Philipoussis, A. Husser, and H. P. Herzig: *Opt. Eng.* **37** (1998) 1804.
- 7) C. W. Mclaughlin: *Proc. IEEE* **90** (2002) 521.
- 8) Y. Mikami, Y. Nagae, Y. Mori, K. Kuwabara, T. Saito, H. Hayama, H. Asada, Y. Akimoto, M. Kobayashi, S. Okazaki, K. Asaka, H. Matsui, K. Nakamura, and E. Kaneko: *IEEE Trans. Electron Devices* **41** (1994) 306.
- 9) S. Ahn, J. Cha, H. Myung, S. Kim, and S. Kang: *Appl. Phys. Lett.* **89** (2006) 213101.
- 10) S. Möller and S. R. Forrest: *J. Appl. Phys.* **91** (2002) 3324.
- 11) H. W. Choi, C. Liu, E. Gu, G. McConnell, J. M. Girkin, I. M. Watson, and M. D. Dawson: *Appl. Phys. Lett.* **84** (2004) 2253.
- 12) M. K. Wei and I. L. Su: *Opt. Express* **12** (2004) 5777.
- 13) E. H. Park, M. J. Kim, and Y. S. Kwon: *IEEE Photonics Technol. Lett.* **11** (1999) 439.
- 14) S. R. Cho, J. Kim, K. S. Oh, S. K. Yang, J. M. Baek, D. H. Jang, T. I. Kim, and H. Jeon: *IEEE Photonics Technol. Lett.* **14** (2002) 378.
- 15) M. Wei, I. Su, Y. Chen, M. Chang, H. Lin, and T. Wu: *J. Micromech. Microeng.* **16** (2006) 368.
- 16) S. Kim and S. Kang: *J. Phys. D* **36** (2003) 2451.
- 17) J. Lee, X. Zhu, Y. Lin, Z. Ge, W. K. Choi, K. Chen, M. Wei, and S. Wu: *SID Int. Symp. Dig. Tech. Pap.* **37** (2006) 68.